NH Tautomerism in the Dimethyl Ester of Bonellin, a Natural Chlorin

Juho Helaja,[†,‡] Franz-Peter Montforts,[§] Ilkka Kilpeläinen,[‡] and Paavo H. Hynninen*[,†]

Department of Chemistry and Institute of Biotechnology, University of Helsinki, FIN-00014 Helsinki, Finland, and Institute of Organic Chemistry, University of Bremen, Leobener Str. NW 2, P.O. Box 33 04 40, D-28359 Bremen, Germany

Received June 29, 1998

The NH protons of the chlorins (17,18-dihydroporphyrins) and fully conjugated porphyrins can undergo tautomerization between the four central nitrogens. We have investigated the NH tautomerization process of bonellin dimethyl ester by NMR spectroscopy and molecular modeling. In this natural chlorin derivative, the tautomerization was observed to occur between the two degenerate $N^{21}-H$, $N^{23}-H$ *trans*-tautomers. The dynamic ^1H NMR measurements showed a coalescence temperature of 297 K for the total tautomeric exchange process ($N^{21}-H_a \rightleftharpoons N^{23}-H_b$). The free energy of activation $\Delta G_{297}^{\ddagger}$ was calculated to be 14.4 kcal/mol on the basis of the Eyring equation. The two-dimensional ^1H and ^{15}N heteronuclear single quantum coherence (HSQC) and heteronuclear multiple bond correlation (HMBC) NMR techniques were used to assign the ^{15}N and NH proton resonances at natural abundance. In addition to the strong $^{15}N-^1H$ one-bond correlations, the HSQC spectrum showed weak correlations between the diagonally opposite nitrogen and proton, thus providing clear evidence for the NH tautomeric exchange. These weak correlations arise from the exchange between the NH protons after the refocusing period of the HSQC pulse sequence. The semiempirical molecular modeling methods AM1 and PM3 were used to estimate the energies of the possible tautomers. The AM1 and PM3 methods with an unrestricted Hartree−Fock (UHF) spin-pairing option both favor strongly the chlorin tautomers in which an aromatic 18-atom 18 π-electron delocalization pathway is possible without delocalizing the lone-pair electrons of N^{24} in the reduced sub-ring. In the proposed tautomerization pathway, the fully aromatic $N^{21}-H$, $N^{22}-H$ and $N^{22}-H$, $N^{23}-H$ *cis*-tautomers were found to be energetically more advantageous than the less aromatic $N^{21}-H$, $N^{24}-H$ and $N^{23}-H$, $N^{24}-H$ *cis*-tautomers. The stepwise tautomerization mechanism is concluded for the proton transfer.

The application of naturally occurring bonellin[1] (**1**) and other chlorins[2] as potential sensitizers for photodynamic tumor therapy of cancer (PDT) and photodynamic treatment of infectious diseases requires the exact determination of structures to ensure defined structure−effect relationships. This aspect is also addressed by the

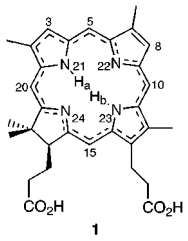

1

national drug administration offices on approval and registration of new drugs. Though the construction and configuration of bonellin have been undoubtedly assigned,[1,3] less attention has been paid to the potential existence of NH tautomers of bonellin and other chlorin structures.

Only a few NH tautomerism studies on chlorins (17,18-dihydroporphyrins) have been reported to date.[4−7] In contrast, the NH tautomerism of fully conjugated porphyrins has been investigated with several variously substituted porphyrins using NMR and IR spectroscopies and molecular modeling.[8−14] It is nowadays agreed that the tautomerization process occurs with a stepwise mechanism via the *cis*-tautomer intermediates, in which the NH protons are located at adjacent nitrogens.[11,12]

It has been concluded on the basis of dynamic NMR studies that all nonsymmetric free-base porphyrins exist in solution as a mixture of two distinct *trans*-NH tautomers possessing different energies and, hence, different populations.[8,10] The two distinct *trans*-tautomers have

† Department of Chemistry, P.O. Box 55, University of Helsinki.
‡ Institute of Biotechnology, P.O. Box 56, University of Helsinki.
§ Institute of Organic Chemistry, FB2, University of Bremen.

(1) Montforts, F.-P.; Müller, C. M.; Lincke, A. *Liebigs Ann. Chem.* **1990**, 415.
(2) Bonnett, R. *Chem. Soc. Rev.* **1995**, *24*, 19.
(3) Montforts, F.-P.; Schwartz, U. M. *Liebigs Ann. Chem.* **1991**, 709.
(4) Storm, C. B.; Teklu, Y. *J. Am. Chem. Soc.* **1972**, *94*, 1745.
(5) Schlabach, M.; Scherer, G.; Limbach, H.-H. *J. Am. Chem. Soc.* **1991**, *113*, 3550.
(6) Bonnett, R.; Djelal, B. D.; Hawkes, G. E.; Haycock, P.; Pont, F. *J. Chem. Soc., Perkin Trans. 2* **1994**, 1839.
(7) Almlöf, J.; Fischer, T. H.; Gassman, P. G.; Ghosh, A.; Häser, M. *J. Phys. Chem.* **1993**, *97*, 10964.
(8) Crossley, M. J.; Field, L. D.; Harding, M. M.; Sternhell, S. *J. Am. Chem. Soc.* **1987**, *109*, 2335.
(9) Crossley, M. J.; Harding, M. M.; Sternhell, S. *J. Org. Chem.* **1988**, *53*, 1132.
(10) Crossley, M. J.; Harding, M. M.; Sternhell, S. *J. Org. Chem.* **1992**, *57*, 1883.
(11) Braun, J.; Schlabach, M.; Wehrle, B.; Köcher, M.; Vogel, E.; Limbach, H.-H. *J. Am. Chem. Soc.* **1994**, *116*, 6593 and references therein.
(12) Ghosh, A.; Almlöf, J. *J. Phys. Chem.* **1995**, *99*, 1073 and references therein.
(13) Reimers, J. R.; Lü, T. X.; Crossley, M. J.; Hush, N. S. *J. Am. Chem. Soc.* **1995**, *177*, 2855.
(14) Merz, K. M., Jr.; Reynolds, C. H. *J. Chem. Soc., Chem. Commun.* **1988**, 90.

10.1021/jo981260q CCC: $18.00
Published on Web 12/30/1998

Scheme 1

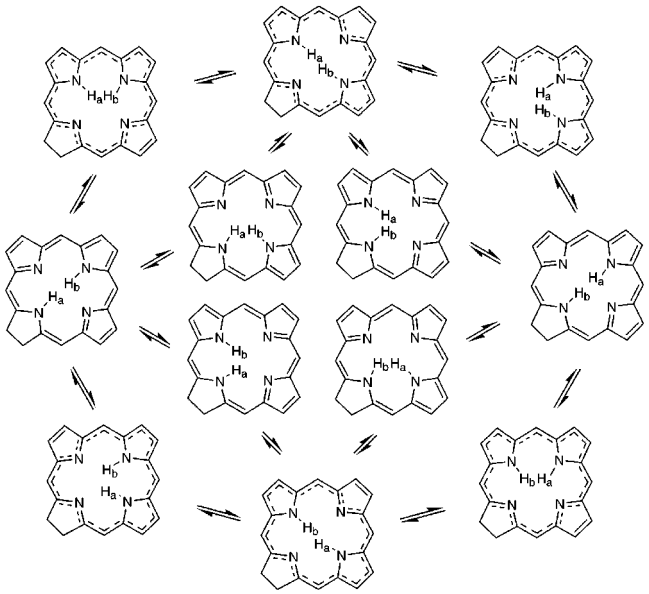

been observed for unsymmetrically substituted *meso*-tetraphenylporphyrins, one with a major and another with a minor population.[8,10] Two values, $\Delta G_1^{\ddagger}$ and $\Delta G_2^{\ddagger}$, for the free energy of activation were determined, and a preferred directionality of proton transfer was deduced for the tautomeric exchange in the porphyrins using ^{1}H NMR line-shape analysis of the NH protons.[8] For symmetrically substituted porphyrins, the two pairs of *trans*-NH tautomers in which the two inner hydrogens reside on the diagonally opposite nitrogens are degenerate and, hence, occur in the tautomeric mixture in equal amounts. Therefore, they cannot be separately detected by spectroscopic methods. In the case of chlorins, there is only one pair of stable *trans*-tautomers (**2a** and **2b**), in which

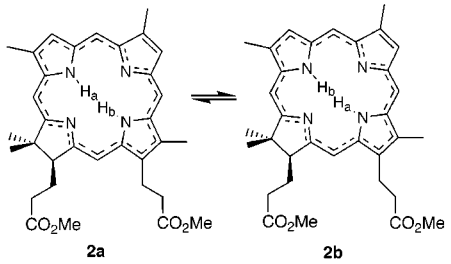

2a **2b**

the central hydrogens are residing on N^{21} and N^{23}. The other *trans*-tautomers and *cis*-tautomers (Scheme 1), where one hydrogen atom occupies the N-atom of the reduced ring, are expected to be of considerably higher energy, because such configurations interrupt the 18-atom [18]-diazaannulene delocalization pathway, unless the lone-pair electrons of N^{24} are delocalized. (This can be predicted to require several kcal/mol; cf. the resonance energies (RE) of pyrrole, pyridine, and benzene, RE = 22, 28, and 36 kcal/mol, respectively.) All possible chlorin tautomers and NH exchange pathways are shown in Scheme 1. The broken-line structures represent the aromatic *trans*- and *cis*-tautomers, in which the [18]-diazaannulene delocalization pathway is maintained without delocalizing the lone-pair electrons of N^{24}.

In a study of *meso*-tetraphenylchlorin, only one pair of degenerate tautomers was observed, and a stepwise tautomerization mechanism was proposed on the basis of kinetic theory of HH/DH/DD isotope effects.[5] Also, the self-consistent-field (SCF) theory, using both ab initio and semiempirical molecular modeling methods, supports the stepwise mechanism for the NH tautomerization in fully conjugated porphyrins.[12−14] Those calculations have predicted that the spectroscopically invisible *cis*-tautomers are energetically quite close to the *trans*-tautomers. The calculated energies for the transition states (TS) between the tautomers suggest that the mechanism is asynchronous for the NH tautomerism in the porphyrins.[13]

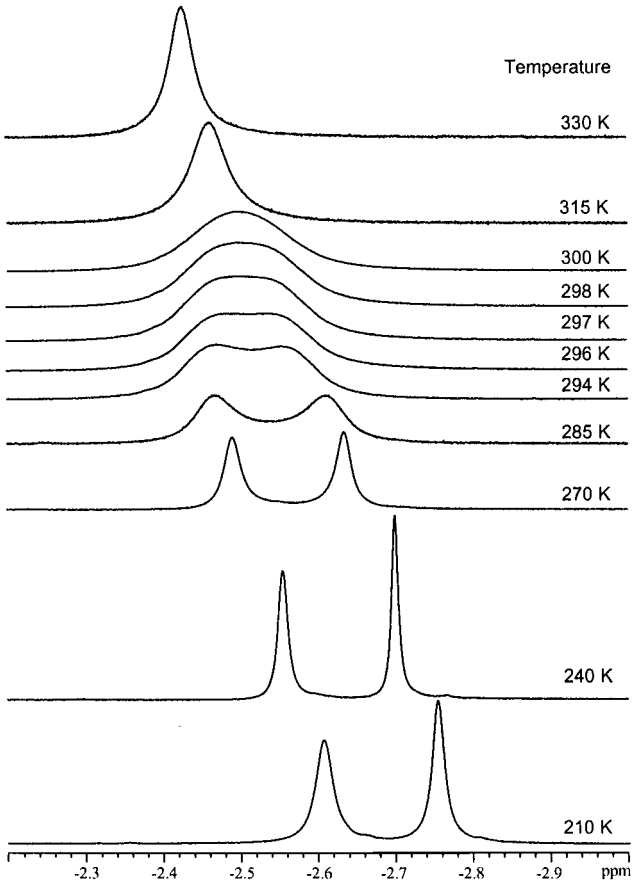

Figure 1. NH section of the ^{1}H NMR spectrum of bonellin DME in $CDCl_3$ at various temperatures.

In this article, we describe the results from our investigations on the NH tautomerism of bonellin dimethyl ester (DME) (Figure 1) using semiempirical AM1 and PM3 molecular modeling methods and dynamic NMR spectroscopy including ^{1}H−^{15}N heteronuclear single quantum coherence (HSQC) and heteronuclear multiple bond correlation (HMBC) NMR experiments.

Results

The variable-temperature NH proton NMR spectra of bonellin DME are shown in Figure 1. The temperature dependence of the NH proton signals clearly indicates NH tautomerism. At low temperatures, two narrow separate signals are observed. When the temperature is raised, the signals merge at 297 K, which hence represents the coalescence temperature, T_c. On raising the temperature of the sample further, the broad signal becomes narrower. The energy barrier for the total tautomeric exchange process can be calculated from the

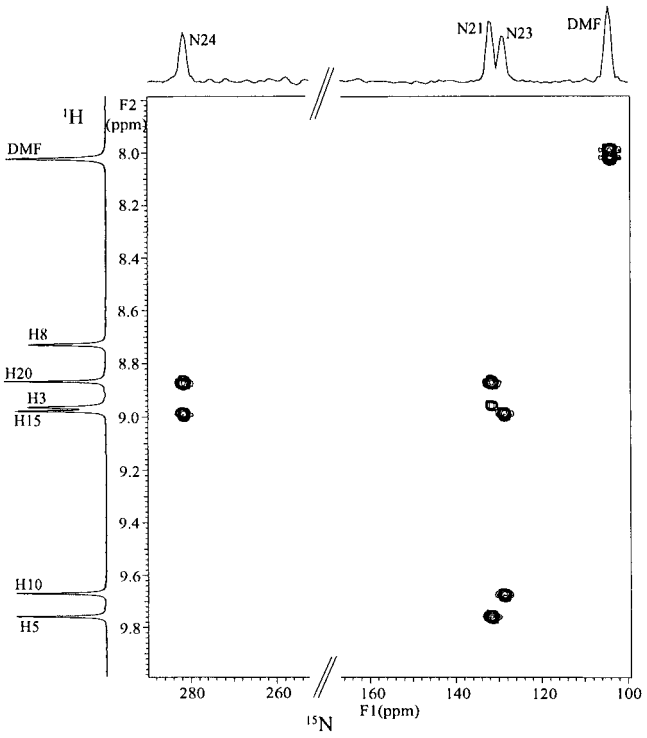

Figure 2. ^{1}H−^{15}N HMBC NMR spectrum of bonellin DME at 278 K.

Eyring equation,[15,16] $\Delta G_c^{\ddagger} = 4.58T_c(10.32 + \log T_c/k_c)$ cal/mol. The exchange rate constant (k_c) at the coalescence temperature is obtained from the equation, $k_c = \pi\,\Delta\nu/\sqrt{2}$, where $\Delta\nu$ is the separation between the two signals when there is no chemical exchange (T = 210 K). The insertion of 297 K for T_c and 74 Hz for $\Delta\nu$ (the measured line separation in the absence of exchange) in the above equations gives $\Delta G_c^{\ddagger} = 14.4$ kcal/mol (60.2 kJ/mol), which represents the Gibbs free energy of activation for the total tautomeric exchange process, **2a** ⇌ **2b**.

Dynamic measurements were also performed down to 180 K using CD_2Cl_2 as solvent to trace possible tautomers separated by low-energy barriers (Scheme 1). However, below 210 K, the proton signals experienced general broadening, which obscured the behavior of the NH proton signals. Furthermore, it can be noticed from the dynamic ^{1}H spectra that the chemical shifts of the NH protons (Figure 1) are shifted to higher field ($\Delta\delta_H$ = −0.25), whereas the methine protons of the chlorin ring are deshielded ($\Delta\delta_H$ = 0.08−0.15), when the temperature decreases from 330 to 210 K. These effects originate from an increase of aromatic ring current in the chlorin ring. The strengthening of the ring current can arise from the following factors: (1) the most aromatic and, hence, most stable chlorin NH tautomer (Figure 4, A) is more populated than the less aromatic NH tautomers (Figure 4, B−D) at low temperatures; and (2) the dynamic deformations of the chlorin macrocycle are damped out, which increases the planarity and, consequently, the aromaticity of the chlorin ring at low temperatures. The uniform deshielding of the methine protons in the chlorin macrocycle indicates that intermolecular $\pi-\pi$ interaction effects are not involved.[17,18]

(15) Sandström, J. *Dynamic NMR Spectroscopy*; Academic Press: London, 1982; pp 79 and 96.
(16) Friebolin, H. *Basic One- and Two-Dimensional NMR Spectroscopy*; VCH: Weinheim, 1993; p 295.

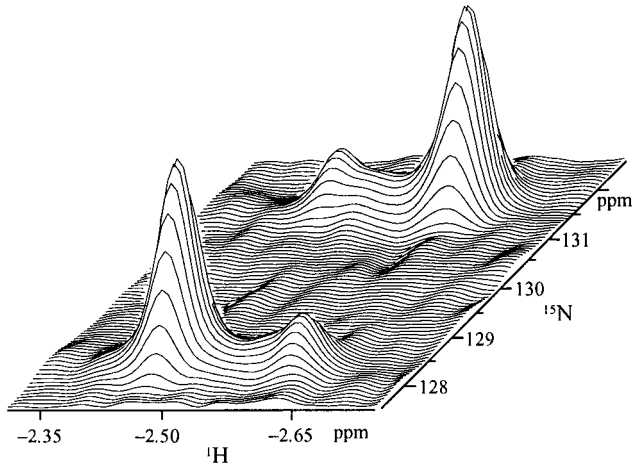

Figure 3. ^{1}H−^{15}N HSQC NMR spectrum of bonellin DME at 278 K.

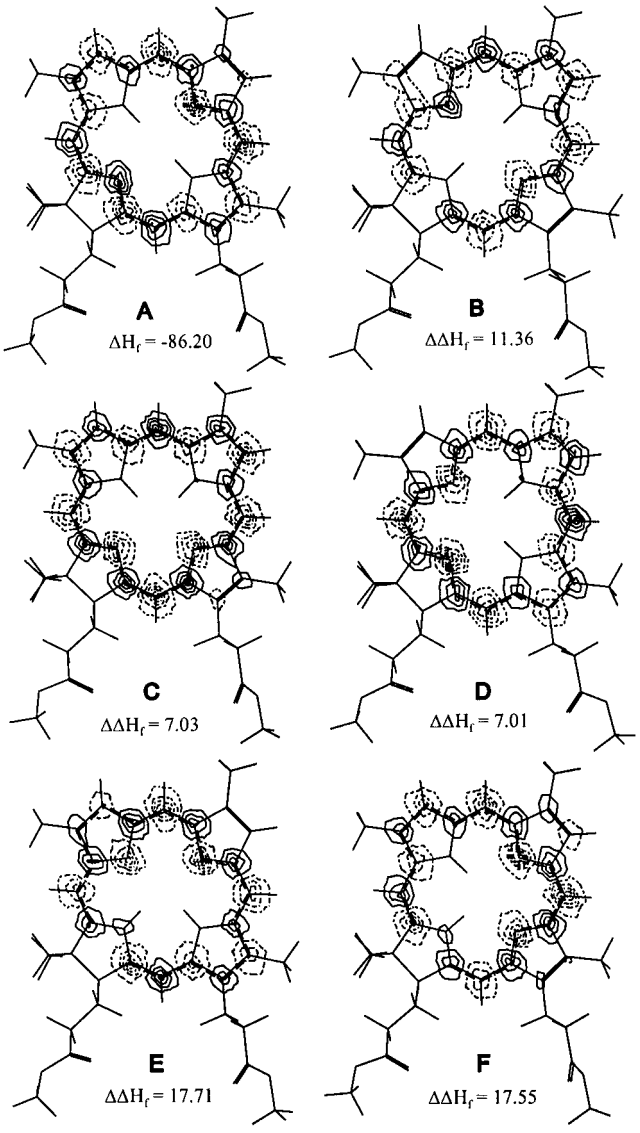

Figure 4. PM3−UHF optimized NH tautomer structures of bonellin DME with spin-density contour maps. Broken and unbroken contour lines indicate opposite phases of polarized spins.

The ^{1}H−^{15}N heteronuclear NMR experiments were carried out at the natural abundance of ^{15}N. In the

Table 1. AM1 and PM3 (RHF/UHF) Optimized Heat of Formation (ΔH_f) Values of the Most Stable *trans* Tautomer of Bonellin DME (A) and the Relative Energies of the Other Tautomers (B−F)

	ΔH_f of **A** and the $\Delta\Delta H_f$ [(**B**, **C**, **D**, **E**, or **F**) − (**A**)] in kcal/mol			
	AM1		PM3	
NH tautomer	RHF	UHF	RHF	UHF
$N^{21,23}$(**A**)	−19.45	−40.56	−68.90	−86.20
$N^{22,24}$(**B**)	0.55	9.59	1.08	11.36
$N^{21,22}$(**C**)	5.44	6.05	5.75	7.03
$N^{22,23}$(**D**)	5.87	6.32	5.75	7.01
$N^{23,24}$(**E**)	8.65	17.35	7.98	17.71
$N^{21,24}$(**F**)	8.32	17.15	7.89	17.55

HMBC[19] spectra at 278 K, correlation signals for the chlorin *meso*-CH protons were found for three central nitrogens with different frequencies (Figure 2). On the basis of these correlations, nitrogens N^{21} (131.5 ppm), N^{23} (128.5 ppm), and N^{24} (281.5 ppm) could be reliably assigned. In contrast, no HMBC correlation(s) were observed for N^{22} of ring B in the temperature range of 278−320 K. The $^1H-^{15}N$ HSQC[20,21] spectrum at 278 K (Figure 3) showed a pair of strong correlation peaks ($\delta_H = -2.48$ and -2.63; $\delta_N = 128.5$ and 131.5) and another pair of weak correlations with the same δ_H and δ_N values. The strong peaks represent the one-bond $^1H-^{15}N$ correlations arising from the predominant *trans*-tautomer (**2a**), in which the two inner protons, H_a and H_b, reside on N^{21} and N^{23}, respectively. The weak correlation peaks can be assigned to the degenerate *trans*-tautomer (**2b**), with H_a at N^{23} and H_b at N^{21}, which was formed after the refocusing period of the HSQC pulse sequence[20,21] as a result from the NH tautomeric exchange, which is relatively fast on the NMR time scale (ms). These results from the HSQC experiment demonstrate in a convincing manner that NH tautomerization occurs in chlorins, and they also provide significant information regarding the dynamics and mechanism of the tautomeric process in these compounds.

The semiempirical molecular modeling methods Austin Model 1 (AM1)[22] and Parametric Method 3 (PM3)[23] with unrestricted and restricted Hartree−Fock (UHF and RHF) spin-pairing were used to optimize the structures for the six possible bonellin NH tautomers. The calculated energies of the tautomers are listed in Table 1. The UHF calculations give clearly higher energies for all tautomers compared with the corresponding energies obtained by the RHF method. In particular, for the N^{24} protonated tautomers, in which the fully aromatic 18 π-electron pathway is interrupted, the UHF energies are remarkably higher (9−10 kcal/mol) than the corresponding RHF energies. On the other hand, the energy differences between the RHF and UHF optimized structures are relatively small for all fully aromatic tautomers (0.5−1.5 kcal/mol).

The macrocyclic chlorin ring was planar in all PM3 optimized structures of the bonellin tautomers. With the UHF option, the NH protons also were in the plane for all tautomers. In the PM3−RHF optimized structures, the NH protons were slightly bent out of the plane for all *cis*-tautomers. From the AM1−UHF and AM1−RHF optimized structures, only the *trans*-NH tautomers were planar. Moreover, one pyrrolic sub-ring with an NH group was bent out of the plane in all AM1 optimized *cis*-tautomer structures. This behavior was stronger with the RHF option than with the UHF.

The spin-density maps of the PM3−UHF structures in Figure 4 indicate spin-polarization of the delocalized electrons. These maps show visually how the aromatic 18 π-electron pathway in the chlorin ring is changed depending on the NH tautomer. It is noteworthy that the delocalization pathway is interrupted in all tautomers in which a hydrogen atom occupies the N^{24} of the reduced sub-ring, unless the lone-pair electrons of N^{24} are delocalized. Apparently, the data on the C−C and C−N bond-length alterations in different chlorin tautomers would give similar information, but the variations in the spin-density maps can be more easily perceived and interpreted. The higher energies obtained for the less aromatic *cis*-tautomers E and F (Figure 4) suggest that these are energetically unfavorable intermediates in the tautomeric process. It should be noted, in addition, that the fully aromatic *cis*-tautomers C and D have lower energy than the less aromatic *trans*-tautomer B (Figure 4).

Discussion

It can be expected that in the NH proton transfer pathway of chlorin (Scheme 1) the less aromatic tautomers are energetically less favorable than the fully aromatic ones. This hypothesis is in accordance with the tautomer energies (Table 1) obtained for the bonellin DME by the AM1 and PM3 methods with the UHF optimization. In contrast, when the RHF optimization is used, only a small difference is observed between the energies of the fully aromatic and less aromatic tautomers. Because there is forced spin-pairing in the RHF method, it does not count the delocalization energies of electrons as well as the UHF method does. Therefore, only the more realistic UHF optimized tautomer energies will be considered in the following discussion.

When optimizing structures for fully conjugated porphyrins, it has been shown that the PM3−UHF method gives $\Delta\Delta H_f$ values and symmetry properties that are qualitatively similar to those obtained by the ab initio MP2 method.[13] Nevertheless, the PM3−UHF optimized NH tautomer structures of the porphyrins showed higher symmetry than the structures optimized using the AM1−UHF method.[13] In our study of the bonellin DME NH tautomers, both the AM1− and PM3−UHF methods afforded optimized structures with similar symmetry properties when the planarity of chlorin ring was used as a measure of symmetry.

The $\Delta\Delta H_f$ value of a single NH tautomer can be considered to consist of two separate factors. One originates from the repulsion energy between the adjacent NH protons (*cis*-tautomers) and another from the decrease in the delocalization (resonance) energy of the NH tautomers, which do not possess the preferred 18-atom [18]-22,24-diazaannulene delocalization pathway. The decrease of the delocalization energy is highest for the

(17) Hunter, C. A.; Sanders, J. K. M. *J. Am. Chem. Soc.* **1990**, *112*, 5525.
(18) Hynninen, P. H.; Lötjönen, S. *Biochim. Biophys. Acta* **1993**, *1083*, 374.
(19) Summers, M. F.; Marzilli, L. G.; Bax, A. *J. Am. Chem. Soc.* **1987**, *109*, 566.
(20) Bodenhausen, G.; Ruben, D. J. *Chem. Phys. Lett.* **1980**, *69*, 185.
(21) Kay, L. E.; Keifer, P.; Saarinen, T. *J. Am. Chem. Soc.* **1992**, *114*, 10663.
(22) Dewar, M. J. S.; Zoebisch, E. G.; Healy, E. F.; Stewart, J. J. P. *J. Am. Chem. Soc.* **1985**, *107*, 3902.
(23) Stewart, J. J. P. *J. Comput. Chem.* **1989**, *10*, 208.

N^{24} protonated cis- and *trans*-tautomers, in which the delocalization of the lone-pair electrons of N^{24} is required to maintain the 18-atom [18]-electron delocalization pathway in the chlorin ring. The comparison of the resonance energies of pyrrole, pyridine, and benzene (22, 28, and 36 kcal/mol,[24] respectively) indicates that the delocalization of one nitrogen electron takes 6−8 kcal/mol. The highest $\Delta\Delta H_f$ values (ca. 17.5 kcal/mol) obtained for the E and F *cis*-tautomers (Figure 4) compare well with the above energy values for the delocalization of one electron, as two N^{24} electrons must be delocalized to maintain aromaticity in the chlorin ring.

In principle, there are eight possible routes in the NH proton-transfer pathway of chlorin (Scheme 1) to achieve the total tautomeric exchange, $N^{21}-H_a \rightleftharpoons N^{23}-H_b$. The high $\Delta\Delta H_f$ values (ca. 10.5 kcal/mol) obtained by the AM1− and PM3−UHF methods for the less aromatic *cis*-tautomers E and F relative to the more aromatic *cis*-tautomers C and D (Table 1, Figure 4) indicate that the former tautomers are improbable intermediates in the NH proton transfer of bonellin DME. This leads us to the conclusion that the energetically advantageous proton transfer proceeds via the peripheral tautomers in Scheme 1. The AM1− and PM3−UHF methods give $\Delta\Delta H_f$ values of 6 and 7 kcal/mol for the more aromatic *cis*-tautomers C and D, and the $\Delta\Delta H_f$ values for the less aromatic *trans*-tautomer B are 9.6 and 11.4 kcal/mol, respectively, relative to the most stable and aromatic *trans*-tautomer A (Table 1).

The lack of long-range HMBC correlations between the N^{22} nitrogen and the CH protons at positions 5, 8, or 10 suggests that the N^{22} signal is broadened below the detection limit of the experiment. According to our interpretation, the $N^{21}-H_a$ and $N^{23}-H_b$ protons visit the N^{22} nitrogen for such periods of time relative to the NMR time scale that the N^{22} signal is line-broadened beyond visibility. The ^{15}N chemical shift of the nonprotonated N^{22} should be near the δ_N value of the nonprotonated N^{24} (281.5 ppm), and that of the protonated N^{22} is expected to be close to the δ_N values of the protonated N^{21} and N^{23} (131.5 and 128.5 ppm, respectively). As the δ_N values of the nonprotonated and protonated N^{22} can differ up to 150 ppm, the line-broadening of the N^{22} signal is expected when the NH proton exchange rate is comparable to the NMR time scale. It seems that the NH protons are most of the time bound to N^{21} and N^{23} nitrogens but make short visits to the N^{22} nitrogen. Thus, the absence of the HMBC correlation signal for N^{22} has diagnostic value, providing clear evidence for the occurrence of the C and D *cis*-tautomers as intermediates. This evidence supports strongly the conclusion that the overall tautomeric process to accomplish the NH exchange between the degenerate tautomers, **2a** ⇌ **2b**, takes place in a stepwise fashion (asynchronously) via the peripheral tautomers in Scheme 1. The result of the overall tautomeric process can be observed in the HSQC spectrum (Figure 3).

The calculated free energy of activation, $\Delta G_{297}^{\ddagger} = 14.4$ kcal/mol, for the total NH tautomeric exchange, **2a** ⇌ **2b**, is determined by the highest and hence the rate-limiting energy barrier in the tautomeric process. In the peripheral tautomerization pathway (Scheme 1), the highest energy barrier is equivalent to the energy of the TS between intermediate C (or D) and the highest-energy intermediate B (Figure 4). This can be concluded on the basis of the Hammond postulate, which states that for any single reaction step the geometry of the TS for that step resembles the side to which it is closer in free energy.[25] For the symmetrically substituted, fully conjugated porphyrins, a synchronous tautomerization mechanism has been postulated.[4,26−28] In the case of chlorins, the synchronous H_a and H_b transfer between the adjacent *trans*-tautomers A and B (Figure 4) would be impossible even in principle, because the asymmetry of the 17,18-dihydroporphyrin macrocycle most likely would imply that also the energy barrier for the H_a and H_b reaction coordinates also is asymmetric.

In conclusion, the NMR and molecular modeling results both suggest that the less aromatic *cis* NH tautomers (central tautomers in Scheme 1) are not significantly involved in the NH tautomeric process of bonellin DME. Hence, we conclude that the overall tautomerization proceeds via the fully aromatic *cis*-tautomers and the less aromatic *trans*-tautomer (peripheral tautomers in Scheme 1) according to a stepwise mechanism.

Experimental Section

NMR Spectra. The isolation and purification of the natural bonellin and its methylation have been described elsewhere.[1] All NMR spectra were recorded on a Varian Unity 500 spectrometer. The ^1H spectra were measured from 8 mg of bonellin DME in 0.6 mL $CDCl_3$ (Fluka, 99.95% D, ampule or bottle stabilized with silver foil, stored at 277 K) in a 5 mm NMR tube and referenced to internal TMS (0.00 ppm) (99.9%, Cambridge Isotope Laboratories). The coalescence temperature remained constant when CD_2Cl_2 (Merck 99.8% D, ampule) was used instead of $CDCl_3$. The ^1H signals of methanol and ethylene glycol (100%, Varian test samples) were used for low- and high-temperature calibrations, respectively.

The $^1H-^{15}N$ NMR heteronuclear correlation spectra were measured from a sample prepared by dissolving 8 mg of bonellin DME in 0.2 mL $CDCl_3$ (purity as above) in a 5 mm Shigemi tube. A small amount (ca. 1 μL) of DMF (Merck, 99.5%, dried with 4 Å molecular sieves, BDH) was used as internal standard (δ_N 103.8) for the ^{15}N chemical shifts in the HMBC experiment. The addition of DMF did not noticeably affect the proton chemical shifts of bonellin DME. Also the $\Delta\delta_N$ values of the $^1H-^{15}N$ HMBC correlation peaks were the same with or without DMF. The coherence selection in the HMBC pulse sequence[19,29] was achieved by applying two 1 ms gradient pulses with a gradient ratio of 10/−9 along the *z*-axis field. The first gradient pulse was placed after the ^1H 180° pulse and the second one after the last ^{15}N 90° pulse. In the HMBC experiment, the spectral width was set to 7 kHz in F2 and to 15 kHz in F1, the number of transients was 48, and 300 time increments were acquired with an acquisition time of 0.22 s. The data were zero-filled to give a 2 × 4K × 2K data matrix. The HSQC pulse sequence was a gradient-enhanced modification of Kay et al.[21] In the HSQC experiment, the spectral width was set to 7 kHz in F2 and to 3 kHz in F1, the number of transients was 80, and 128 time increments were acquired with an acquisition time of 0.08 s. The data were zero-filled to give a 2 × 4K × 2K data matrix. A relaxation delay of 1 s was used in all experiments between the acquired transients. All data in the 2D experiments were collected using the hypercomplex method.

(24) Ege, S. N. *Organic Chemistry, Structure and Reactivity*; D. C. Heath and Company: Lexington, 1994; p 1061.

(25) March, J. *Advanced Organic Chemistry*, 4th ed.; Wiley: New York, 1992; p 215.

(26) Eaton, S. S.; Eaton, G. R. *J. Am. Chem. Soc.* **1977**, *99*, 1601.

(27) Henning, J.; Limbach, H.-H. *J. Chem. Soc., Faraday Trans. 2* **1979**, *75*, 752.

(28) Limbach, H.-H.; Henning, J. *J. Chem. Phys.* **1979**, *71*, 3120.

(29) Kilpeläinen, I.; Kaltia, S.; Kuronen, P.; Hyvärinen, K.; Hynninen, P. H. *Magn. Reson. Chem.* **1994**, *32*, 29.

Molecular Modeling. The AM1[22] and PM3[23] molecular modelings were performed on a Pentium Pro 200 MHz PC computer using the HyperChem (4.5) software package (Hypercube, Waterloo, ON, Canada) for molecular modeling. The full optimization of geometry was achieved for the NH tautomers of bonellin DME using 202 molecular orbitals in the semiempirical calculations. The structures were energy-optimized employing the Polak−Ribiere conjugate gradient optimization algorithm with an energy convergence criterion of 0.01 kcal $Å^{-1}$ mol^{-1}.

Acknowledgment. Support from the Academy of Finland and Deutscher Akademischer Austauschdienst (DAAD) is acknowledged.

JO981260Q